strong preference for the latter at equilibrium.

Acknowledgment. We thank Dr. M. Peterson for enlightening discussions. Financial support by the Natural Sciences and Engineering Research Council of Canada and time donated by the Ontario Centre for Large Scale Computation on the CRAY X-MP/24 supercomputer and by the Computer Centre of Scarborough College on the SUN 3260 minicomputer is gratefully acknowledged.

Registry No. 1, 463-51-4; **4**, 50-00-0; **5**, 67285-39-6; **10**, 124098-83-5; **11**, 124098-84-6.

Series of Two-Coordinate and Quasi-Two-Coordinate Transition-Metal Complexes: Synthesis, Structural, and Spectroscopic Studies of Sterically Demanding Borylamide Ligands $-NRBR'_2$ (R = Ph, R' = Mes, Xyl; R = R' = Mes), Their Lithium Salts $Li(Et_2O)_2NRBR'_2$, and Their Transition-Metal Derivatives $M(NPhBMes_2)_2$ (M = Cr, Co, Ni), $Co(NPhBXyl_2)_2$, and $M(NMesBMes_2)_2$ (M = Cr → Ni)

Hong Chen, Ruth A. Bartlett, Marilyn M. Olmstead, Philip P. Power,* and Steven C. Shoner

Contribution from the Department of Chemistry, University of California, Davis, California 95616. *Received June 26, 1989*

Abstract: Amide ligands, modified by the presence of the diarylboryl substituents $-BMes_2$ or $-BXyl_2$ (Mes = 2,4,6-$Me_3C_6H_2$, Xyl = 2,6-$Me_2C_6H_3$), have been used to effect the synthesis and characterization of several low-coordinate metal complexes of unusual structure. The synthesis of the aminoboranes $HNRBMes_2$ (R = Ph, **1**; R = Mes, **2**) and $HNPhBXyl_2$ (**1a**), the lithium borylamide salts $Li(Et_2O)_2NRBMes_2$ (R = Ph, **3**; R = Mes, **4**), and 10 transition-metal derivatives, $M(NPhBMes_2)_2$ (M = Cr, **5**; Co, **6**; Ni, **7**), $Co(NPhBXyl_2)_2$ (**6a**), $Co[N(C_6D_5)BMes_2]_2$ (**6b**), and $M(NMesBMes_2)_2$ (M = Cr, **8**; Mn, **9**; Fe, **10**; Co, **11**; Ni, **12**), are reported. The X-ray crystal structures of **2**, **4**–**7**, **10**, and **11** are described and discussed in the context of structures **1**, **3**, **8**, **9**, and **12** reported in preliminary publications. The transition-metal complexes were further characterized by UV/vis and EPR spectroscopy and magnetic data. Variable-temperature ^1H NMR spectroscopy of **6**, **6a**, **6b**, **7**, **11**, and **12** is also reported. The transition-metal complexes **5**–**12** are all high spin with nominally two-coordinate geometries. However, they all display some deviation from linearity. The distortion is most severe for the chromium complexes **5** and **8** (N–Cr–N = 110.8 (1)° and 112.3 (3)°) whereas in Fe, Co, and Ni derivatives of $-NMesBMes_2$ deviation of the NMN angle from 180° is only about 13°. The BN bonds within the ligands are short, and the nitrogen and boron centers are invariably planar. The ligands are, in effect, boron–nitrogen analogues of alkenyls. Instead of association through bridging at the nitrogen centers, moderate (in **5**–**8**) or very weak (in **9**–**12**) intramolecular interactions are observed between the ipso carbons of the $-BMes_2$ groups and the metal centers that may cause the observed structural distortions. Variable-temperature ^1H NMR data on **6**, **6a**, **6b**, and **11** indicate that the M···C ligand interactions are not greater than about 10 kcal mol^{-1} for **6**, **6a**, **6b**, and presumably for **5** and **7**, whereas in the NMes compounds **11** and **12** no M–C interactions could be detected at temperatures as low as 192 K. Crystal data with Mo Kα (λ = 0.71069 Å) radiation at 130 K: **2**, $HNMesBMes_2$, $C_{27}H_{34}BN$, a = 8.200 (1) Å, b = 10.370 (3) Å, c = 15.134 (3) Å, α = 109.38 (2)°, β = 80.96 (2)°, γ = 108.71 (2)°, Z = 2, triclinic, space group $P\bar{1}$, R = 0.063; **4**, $Li(Et_2O)_2NMesBMes_2$, a = 10.927 (4) Å, b = 19.626 (5) Å, c = 31.07 (1) Å, Z = 8, orthorhombic, space group $Pbca$, R = 0.085; **5**, $Cr(NPhBMes_2)_2$, $C_{48}H_{54}B_2CrN_2$, a = 11.344 (2) Å, b = 22.531 (8) Å, c = 16.285 (3) Å, β = 94.95 (1)°, Z = 4, monoclinic, space group $P2_1/c$, R = 0.046; **6**, $Co(NPhBMes_2)_2$, $C_{48}H_{54}B_2CoN_2$, a = 13.454 (3) Å, b = 15.466 (4) Å, c = 23.191 (7) Å, β = 99.82 (2)°, Z = 4, monoclinic, space group $P2_1/n$, R = 0.080; **7**, $Ni(NPhBMes_2)_2$, $C_{48}H_{54}B_2NiN_2$, a = 10.616 (4) Å, b = 12.108 (4) Å, c = 17.578 (4) Å, α = 109.27 (2)°, β = 91.89 (3)°, γ = 103.05 (3)°, Z = 2, triclinic, space group $P\bar{1}$, R = 0.057; **10**, $Fe(NMesBMes_2)_2$, $C_{56}H_{66}B_2FeN_2$, a = 11.462 (5) Å, b = 13.784 (6) Å, c = 15.797 (6) Å, α = 103.35 (3)°, β = 101.51 (3)°, γ = 99.87 (4)°, Z = 2, triclinic, space group $P\bar{1}$, R = 0.045; **11**, $Co(NMesBMes_2)_2$, $C_{54}H_{66}B_2CoN_2$, a = 11.399 (5) Å, b = 13.746 (7) Å, c = 15.852 (7) Å, α = 103.13 (4)°, β = 101.76 (4)°, γ = 99.71 (4)°, Z = 2, triclinic, space group $P\bar{1}$, R = 0.057.

Recent results from a number of laboratories have shown that it is possible to achieve a two-coordinate geometry in some open-shell (d^0–d^9) transition-metal complexes under ambient conditions.[1-8] Hitherto this coordination number had been restricted to transition-metal dihalides at high temperature in the gas phase[9] or to species with a closed-shell (d^{10}) electron configuration, for example, complexes of Pt(0), Cu(I), Ag(I), or Hg(II). However, two early papers[10,11] suggested that the divalent

(1) Nowitzki, B.; Hoppe, R. *Croat. Chem. Acta* **1984**, *57*, 537.
(2) Buttrus, N. H.; Eaborn, C.; Hitchcock, P. B.; Smith, J. D.; Sullivan, A. C. *J. Chem. Soc., Chem. Commun.* **1985**, 1380.
(3) Andersen, R. A.; Haaland, A.; Rypdal, K.; Volden, H. V. *J. Chem. Soc., Chem. Commun.* **1985**, 1807.
(4) Bartlett, R. A.; Feng, X.; Olmstead, M. M.; Power, P. P.; Weese, K. J. *J. Am. Chem. Soc.* **1987**, *109*, 4851.
(5) Bartlett, R. A.; Power, P. P. *J. Am. Chem. Soc.* **1987**, *109*, 7563.
(6) Andersen, R. A.; Faegri, K.; Green, J. C.; Haaland, A.; Lappert, M. F.; Leung, W.-P.; Rypdal, K. *Inorg. Chem.* **1988**, *27*, 1782.
(7) Power, P. P. *Comments Inorg. Chem.* **1989**, *VIII*, 177.
(8) Bartlett, R. A.; Chen, H.; Power, P. P. *Angew. Chem., Int. Ed. Engl.* **1989**, *28*, 316.
(9) Hargittai, M. *Coord. Chem. Rev.* **1988**, *91*, 35.
(10) Bürger, H.; Wannagat, U. *Monatsh. Chem.* **1963**, *94*, 1007.

0002-7863/90/1512-1048$02.50/0

species $M[N(SiMe_3)_2]_2$ (M = Mn, Co, Ni) were probably monomeric (and by implication two-coordinate) at low temperature in the vapor phase as suggested by their low boiling points. This observation received support from cryoscopic data[12] on $Co[N(SiMe_3)_2]_2$ in cyclohexane, which indicated that it was also a monomer in solution. However, subsequent X-ray data for both $Mn[N(SiMe_3)_2]_2$[13,14] and $Co[N(SiMe_3)_2]_2$[14] showed them to be dimers with amide bridges in the solid. Soon afterward the first structural characterization of two-coordinate transition-metal complexes appeared that involved the ionic species $[NiO_2]^{2-}$[1] (X-ray) and the neutral compounds $Mn[C(SiMe_3)_3]_2$ (X-ray)[2] and $Mn(CH_2\text{-}t\text{-}Bu)_2$[3] (vapor electron diffraction). These were followed by the X-ray structures of the two-coordinate iron and cobalt species $M[N(SiMePh_2)_2]_2$.[5] In addition, electron diffraction studies on the original $M[N(SiMe_3)_2]_2$ (M = Mn, Fe, Co)[6] compounds proved that they also were monomeric in the vapor phase.

Attempts to extend the use of the versatile silylamide ligands or bulky alkyl groups to other transition metals have encountered problems. For example, $Ni[N(SiMe_3)_2]_2$ is unstable at room temperature and $Cr[N(SiMe_3)_2]_2$, currently an unknown compound, exists only when complexed with Lewis bases as in *trans*-$[Cr\{N(SiMe_3)_2\}_2(THF)_2]$.[15] Similarly, attempts to characterize homoleptic transition-metal dialkyls other than manganese have not yet afforded well-characterized products. One of the objectives in this laboratory has been the synthesis of the widest possible range of two-coordinate transition-metal compounds to allow comparison of the effects of such coordination across a series. During work on $-NPh_2$[16] complexes it emerged that, in some instances, they possessed greater thermal stability than the corresponding derivatives of $-N(SiMe_3)_2$. This is exemplified in $[Ni(NPh_2)_2]_2$, which is quite stable at ambient temperature,[5] whereas $Ni[N(SiMe_3)_2]_2$ decomposes rapidly. It was thought that if diarylamides such as $-NPh_2$ could be prevented from bridging, they could allow the synthesis of a wider range of stable complexes. The technique of modifying the diarylamide ligand with a boryl substituent was then conceived.[4,17] This prevented bridging by involvement of the nitrogen lone pair in bonding to the empty p orbital on boron. Initial investigations[4,8] concerned the species $M(NMesBMes_2)_2$ (M = Cr, Mn, Ni). A fuller account of this work is now provided involving its extension to the ligand $-NPhBMes_2$ and the metal series chromium to nickel.

Experimental Section

General Procedures. All work was performed by using Schlenk techniques under N_2 or a Vacuum Atmospheres HE 43-2 drybox. Solvents were freshly distilled under N_2 from Na/K or Na/K benzophenone ketyl and degassed twice immediately before use.

Physical Measurements. ^1H and ^{11}B NMR spectra were obtained on a General Electric QE-300 spectrometer. Isotropic shifts were calculated from the relationship $(\Delta H/H_0)_{iso} = (\Delta H/H_0)_{obsd} - (\Delta H/H_0)_{dia}$. Electronic absorption spectra were obtained on a Hewlett-Packard 8450A UV/vis spectrometer. Magnetic moment measurements were performed via Evans' method.[18] EPR data were obtained on a Brucker ER-200D spectrometer operating at 9.43–9.49 GHz. All compounds gave satisfactory C, H, and N analyses.

Starting Materials. The compounds H_2NPh and H_2NMes were distilled off CaH_2 under reduced pressure. Solutions of 1.6 M *n*-BuLi in hexane and $H_2NC_6D_5$ were purchased from Aldrich. Mes_2BF was synthesized by the method of Pelter.[19] $HNPhBMes_2$[4] (and $HN(C_6D_5)BMes_2$), $HNMesBMes_2$,[4] and $Li(Et_2O)_2NPhBMes_2$[4] were synthesized as previously described. $CrCl_2$ (Cerac), $MnBr_2$ (Aldrich), $FeBr_2$ (Cerac), $CoCl_2$ (Aldrich), and $NiBr_2$ (Alfa) were used as received. $CrCl_2(THF)_2$,[20] $MnBr_2(THF)_2$,[21,22] and $NiBr_2{\cdot}^5/_3THF$[20] were synthesized by overnight Soxhlet extraction of the anhydrous metal dihalide with THF and structurally characterized by X-ray crystallography. All compounds gave satisfactory C, H, or N analyses.

Syntheses of Compounds 1a, 4–8, and 10–12. $HNPhBXyl_2$ (1a). 2-Bromo-*m*-xylene (18.5 g, 100 mmol) in THF (60 mL) was added dropwise to Mg turnings (2.4 g, 100 mmol) that had been ground with a mortar and pestle and heated, under vacuum, with a hot air gun. The rate of addition was adjusted to maintain gentle reflux of the Grignard solution. When the addition was complete, the reaction mixture was refluxed for 3 h longer. After cooling, this solution was added dropwise to a solution of $BF_3{\cdot}Et_2O$ (6.39 g, 45 mmol) in Et_2O (25 mL) with cooling in an ice bath. The mixture was then refluxed for 3 h and cooled overnight in a −20 °C freezer. The supernatant liquid was removed via cannula and evaporated to give an off-white solid. This was extracted with 4 × 30 mL of hexane, and the combined extracts were filtered. The volume was reduced to about 20 mL under reduced pressure, and cooling in a −20 °C freezer gave colorless crystals of Xyl_2BF: yield 6.5 g, 60.2%; mp = 68–72 °C.

Xyl_2BF (2.4 g, 10 mmol) in Et_2O (25 mL) was treated dropwise with an Et_2O (25 mL) solution formed from aniline (H_2NPh; 0.93 g, 10 mmol) and a hexane solution of 1.6 M *n*-BuLi (6.25 mL). Stirring was continued for 4 h after which the volatile material was removed under reduced pressure. The residue was extracted with 3 × 25 mL of warm hexane, and the combined extracts were then filtered. The volume of the filtrate was lowered to ca. 20 mL under reduced pressure to give the title compound **1a** as almost colorless, pale yellow crystals: yield 2.6 g, 83%; mp = 96–98 °C.

$Li(Et_2O)_2NMesBMes_2$ (4). $HNMesBMes_2$[4] (0.76 g, 2 mmol) in Et_2O (15 mL) was cooled in an ice bath, treated dropwise with *n*-BuLi (1.6 M in hexane, 1.3 mL), and stirred for 30 min. Filtration and reduction of the volume to ca. 10 mL under reduced pressure and cooling in a −20 °C freezer for 12 h gave $Li(Et_2O)_2NMesBMes_2$ as colorless crystals: yield 80%; mp = 157–163 °C; ^{11}B NMR, δ 30.8.

$Cr(NRBMes_2)_2$ (R = Ph, 5; Mes, 8). A solution of $Li(Et_2O)_2NRBMes_2$, generated in situ from $NHRBMes_2$ (2 mmol, 0.68 g, R = Ph; 0.76 g, R = Mes) in Et_2O (30 mL) at 0 °C, was added dropwise to a suspension of $CrCl_2{\cdot}2THF$ (0.266 g, 1 mmol) in Et_2O (10 mL). The solution slowly became green upon stirring for 5 h. The Et_2O was removed under reduced pressure. The dark green residue was extracted with warm (50 °C) hexane (30 mL), and the solution was filtered. The volume was then reduced to ca. 10 mL. Cooling overnight in a −20 °C freezer gave the product $Cr(NPhBMes_2)_2$ (**5**) as green crystals [yield 0.22 g, 30%; mp = 167–177 °C] and $Cr(NMesBMes_2)_2$ (**8**) as green crystals [yield 0.32 g, 39%; mp = 195–197 °C].

$Co(NRBMes_2)_2$ (R = Ph, 6; Mes, 11). $HNRBMes_2$ (2 mmol, 0.68 g, R = Ph; 0.76 g, R = Mes) in Et_2O (30 mL) was cooled in an ice bath, treated dropwise with *n*-BuLi (1.6 M hexane solution, 1.3 mL), and stirred for 30 min. The solution was added dropwise to $CoCl_2$ (0.13 g, 1 mmol) in Et_2O (10 mL). The mixture slowly became red, for R = Mes, or green, for R = Ph, upon stirring for 2 h at room temperature. The Et_2O was removed under reduced pressure. The residue was extracted with hexane (30 mL), and the solution was filtered. The volume was then reduced to ca. 5 mL under reduced pressure. Cooling overnight in a −20

(11) Bürger, H.; Wannagat, U. *Monatsh. Chem.* **1964**, *95*, 1099.
(12) Bradley, D. C.; Fisher, K. J. *J. Am. Chem. Soc.* **1971**, *93*, 2058.
(13) Bradley, D. C.; Hursthouse, M. B.; Malik, K. M. A.; Moseler, R. *Transition Met. Chem. (Weinheim, Ger.)* **1978**, 3253.
(14) Murray, B. D.; Power, P. P. *Inorg. Chem.* **1984**, *23*, 4584.
(15) Bradley, D. C.; Hursthouse, M. B.; Newing, C. W.; Welch, A. J. *J. Am. Soc., Chem. Commun.* **1972**, 567.
(16) Hope, H.; Olmstead, M. M.; Murray, B. D.; Power, P. P. *J. Am. Chem. Soc.* **1985**, *107*, 712.
(17) The species $LiNMeBMe_2$ has been known for a number of years, and this and related reagents have been reacted further to give mercury and tin complexes. See for example: (a) Fusstetter, H.; Nöth, H. *Chem. Ber.* **1979**, *112*, 3672. (b) Fusstetter, H.; Nöth, H. *Chem. Ber.* **1980**, *113*, 791. (c) Fussletter, H.; Kopietz, G.; Nöth, H. *Chem. Ber.* **1980**, *113*, 728. (d) Nöth, H.; Prigge, H.; Rotsch, A. *Chem. Ber.* **1986**, *119*, 1361. (e) Brandl, A.; Nöth, H. *Chem. Ber.* **1978**, *121*, 1371. In addition to the first structure of a lithium borylamide in ref 4, other structures of lithium borylamides have also been published: (e) Bartlett, R. A.; Chen, H.; Dias, H. V. R.; Olmstead, M. M.; Power, P. P. *J. Am. Chem. Soc.* **1988**, *110*, 446. (f) Paetzold, C.; Pelzer, C.; Boese, R. *Chem. Ber.* **1988**, *121*, 51.
(18) Evans, D. F. *J. Chem. Soc., Dalton Trans.* **1959**, 2005.
(19) We thank Professor Pelter for providing an efficient synthesis of Mes_2BF when the published procedure did not work in our hands. The synthesis of **1a** essentially follows the Pelter route.
(20) Bartlett, R. A.; Murray, B. D.; Olmstead, M. M.; Power, P. P.; Sigel, G. A. Unpublished observations, 1986. Both starting materials, which have been structurally characterized, were synthesized by Soxhlet extraction of the anhydrous metal dihalide with THF. The structure of the pale blue *trans*-$[CrCl_2(THF)_2]$ is square planar with long axial metal–halide interactions. The structure of salmon pink $NiBr_2{\cdot}^5/_3(THF)_2$ consists of infinite chains of edge-bridged *trans*-$NiBr_4(THF)_2$ octahedra with every third nickel missing an axial THF.
(21) Bartlett, R. A.; Murray, B. D.; Olmstead, M. M.; Power, P. P.; Sigel, G. A. Unpublished observations, 1986. $MnBr_2(THF)_2$ was obtained by a procedure identical with that for $MnCl_2(THF)_2$.[22] It has a structure consisting of edge-sharing *trans*-$MnBr_2(THF)_2$ octahedra.
(22) Horvath, B.; Möseler, R.; Horvath, E. G *Z. Anorg. Allg. Chem.* **1979**, *450*, 165.

Table I. Important Bond Distances (Å) and Angles (deg) for $HNRBMes_2$ (R = Ph, **1**; Mes, **2**) and $Li(Et_2O)_2NRBMes_2$ (R = Ph, **3**; Mes, **4**)

	1[a]	2[b]	3[a]	4[b,c]
B-N	1.407 (2)	1.406 (3)	1.385 (3)	1.36 (1)
B-C	1.590 (2)	1.597 (3)	1.614 (3)	1.64 (1)
	1.591 (2)	1.582 (4)	1.615 (3)	1.65 (1)
N-C	1.424 (2)	1.427 (3)	1.402 (3)	1.416 (8)
Li-N			1.943 (3)	1.94 (1)
Li-O (av)			1.933 (4)	1.95 (1)
CBC	122.6 (1)	123.8 (2)	122.0 (2)	121.1 (7)
NBC	120.6 (1)	121.6 (2)	121.6 (2)	124.8 (7)
	116.9 (1)	114.6 (2)	116.3 (2)	114.1 (7)
BNC	130.6 (1)	131.6 (2)	124.4 (2)	123.0 (6)
twist angle between B and N planes	9.8	2.8	8.8	9.8
asym in NBC	3.7	7	5.3	10.7

[a] Data from ref 4. [b] This work. [c] Data for major site occupancy.

°C freezer gave the product $Co(NPhBMes_2)_2$ (**6**) as green crystals [yield 0.37 g, 50%; mp = 85–89 °C] and $Co(NMesBMes_2)_2$ (**11**) as red crystals [yield 0.35 g, 43%, no melting observed up to 310 °C]. Compounds **6a**, **6b**, **7**, **10**, and **12** were synthesized in a similar yield by the same route as **6** and **11**, from $CoCl_2$, $FeBr_2$, or $NiBr_2{}^{.5}/_3THF$ starting materials as required. $Co(NPhBXyl_2)_2$ (**6a**) was isolated as dark green crystals in 70% yield; dec pt >100 °C. Compound **6b** was synthesized by a procedure similar to that for **6** by using $H_2NC_6D_5$ instead of H_2NPh. It has physical properties very similar to those of **6**. $Fe(NMesBMes_2)_2$ (**10**) was obtained as yellow crystals that decompose at 150 °C; yield 0.3 g, 37%. $Ni(NPhBMes_2)_2$ (**7**) was obtained as dark red crystals: yield 0.48 g, 65%, mp = 148 °C. $Ni(NMesBMes_2)_2$ (**12**) was obtained as dark red crystals: yield 0.57 g, 70%; mp = 165 °C.

X-ray Data Collection, Solution, and Refinement of the Structures. All X-ray data were collected with the use of a Syntex $P2_1$ diffractometer equipped with a graphite monochromator and locally modified LT-1 device for low-temperature work. Crystallographic programs used were those of SHELXTL, Version 5, installed on a Data General Eclipse computer. Scattering factors were common sources.[23a] An absorption correction was applied by using the method described in ref 23b. All compounds were coated with a layer of hydrocarbon oil upon removal from the Schlenk tube. A suitable crystal was selected, attached to a glass fiber with silicone grease, and immediately placed in the low-temperature nitrogen stream. Table S1 (supplementary material) summarizes the crystal data and refinement for **2**, **4**, **5-7**, **10**, and **11**. Crystal data and some structural data for **1**, **3**, **8**, **9**, and **12** have been published in a preliminary paper[4] and communication.[8] Information on their structures is also provided here both for completeness and in order to place them in context with respect to the unreported compounds above. The important metric features of the structures of **1–12** are summarized in Tables I–III.

Electronic Absorption and EPR Spectra and Magnetic Measurements. The electronic absorption spectra of compounds **5–12** were recorded in toluene. However, manganese and iron complexes **9** and **10** were observed to have essentially featureless spectra with an increase in intensity toward the higher frequency. The data are summarized in Table IV. The magnetic moments of compounds **5–12** are provided in Table V. These were measured at 297.3 K in C_6D_6/C_6H_6 solution via the Evans method.[18] The shifts were measured relative to the residual C_6H_6 resonance. Samples typically invovled 0.008–0.06 g dissolved in 0.5 mL of solvent, which afforded frequency differences in the range of 160–950 Hz at 300 MHz. Variable-temperature ^1H NMR data from **6**, **6a**, **6b**, **7**, **11**, and **12** were recorded in toluene-d_8.

The EPR spectra of **5–12** were recorded on crystalline samples between 7.5 and 11 K with a typical scan range of (3–5) × 10^3 G. The spectra of the chromium complexes **5** and **8** afforded almost identical spectra, with absorptions at g values of 2.1 and 1.94 for **5** and 2.12 and 1.95 for **8**. The spectrum of **9** is characterized by a multiplicity of absorptions. There are three major features at g 6.9, 2.2, and 1.4 that are split into further peaks, suggesting a considerable number of low-lying energy states in this manganese system. The iron compound features two major absorptions at g 4.02 and 2.08 in addition to a feature at g 1.63 that shows fine structure. The cobalt compound $Co(NPhBMes_2)_2$ (**7**) displays a peak at g 2.11. However, in frozen solution (20% w/w in PhMe) at 11 K a new feature, which has considerable fine structure, appears and is centered at $g \approx 7.75$. The mesityl analogue **11** also has an absorption at g 2.10, but absorptions (possibly a multiplet) with g 1.93, 1.89, 1.84, and 1.74 were also observed. Crystals of nickel compounds **8** and **12** that had been recrystallized twice display very similar spectra with an absorption at g 2.1.

(23) (a) *International Tables for X-Ray Crystallography*; Kynoch press: Birmingham, England, 1974; Vol. IV. (b) Program XABS: Hope, H.; Moezzi, B., University of California, Davis. The program obtains an absorption tensor from F_o–F_c differences. Moezzi, B. Ph.D. Dissertation, University of California, Davis, 1987.

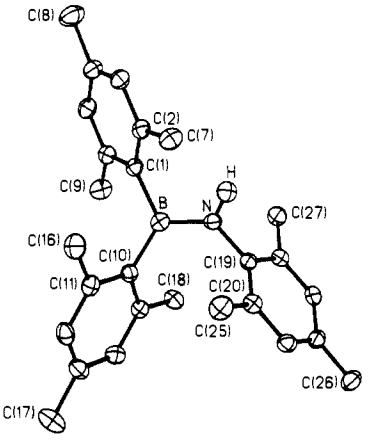

Figure 1. Thermal ellipsoid plot of $NHMesBMes_2$ (**2**). H atoms (except NH) are omitted for clarity. See Table I for details.

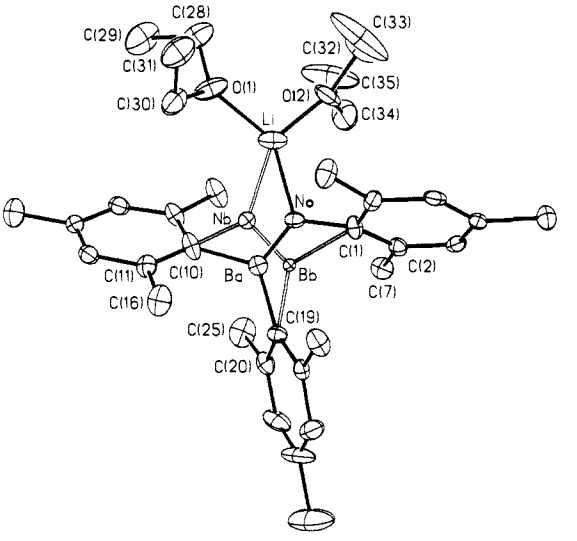

Figure 2. Thermal ellipsoid plot of $Li(Et_2O)_2NMesBMes_2$ (**4**). Site of major (75%) occupancy is indicated by solid lines. H atoms are omitted for clarity. See Table I for details.

Results and Discussion

Structural Descriptions. $HNPhBMes_2$ (1), $HNMesBMes_2$ (2), $Li(Et_2O)_2NPhBMes_2$ (3), and $Li(Et_2O)_2NMesBMes_2$ (4). The important bond distances and angles for these derivatives are summarized in Table I. Structural data for only one of the disordered molecules of **4** are presented. The structures of **1** and **3** were described in a previous publication[4] and are included in Table I for comparison purposes. Compounds **2** and **4** are illustrated in Figures 1 and 2. An obvious feature is that the lithium salts **3** and **4** are monomeric instead of the associated structures normally found in $LiNR_2$ species.[24] In addition, **1–4** possess essentially planar cores of C_2BNCH (or Li) atoms with only small twist angles between the boron and nitrogen planes. The B-N distances are, as expected, significantly shorter than the sum of the covalent radii of boron and nitrogen (1.55–1.58 Å)[25] and vary

(24) Setzer, W. N.; Schleyer, P. v. R. *Adv. Organomet. Chem.* **1985**, *24*, 353. Barr, D.; Clegg, W.; Mulvey, R. E.; Snaith, R. *J. Chem. Soc., Chem. Commun.* **1984**, 469. Barr, D.; Clegg, W.; Mulvey, R. E.; Snaith, R. *J. Chem. Soc., Chem. Commun.* **1984**, 285. Engelhardt, L. M.; May, A. S.; Raston, C. L.; White, A. L. *J. Chem. Soc., Dalton Trans.* **1983**, 1671. Barr, D.; Clegg, W.; Mulvey, R. E.; Smith, R.; Wright, D. S. *J. Chem. Soc., Chem. Commun.* **1987**, 716. Armstrong, D. R.; Barr, D.; Clegg, W.; Mulvey, R. E.; Reed, D.; Snaith, R.; Wade, K. *J. Chem. Soc., Chem. Commun.* **1986**, 869.

Table II. Important Bond Distances (Å) and Angles (deg) and Other Structural Parameters for $M(NPhBMes_2)_2$ (M = Cr, Co, Ni)

	Cr, **5**	Co, **6**	Ni, **7**
N-M-N	110.8 (1)	127.1 (2)	135.7 (1)
M-N (av)	1.982 (2)	1.909 (5)	1.885 (4)
M···C (<2.8 Å)	2.328 (2)	2.388 (6)	2.370 (3)
	2.406 (2)	2.387 (5)	2.402 (4)
B-N (av)	1.389 (3)	1.398 (8)	1.403 (6)
B-C	1.585 (4)	1.596 (9)	1.586 (5)
	1.591 (3)	1.592 (9)	1.575 (7)
B-C(···M)	1.630 (4)	1.639 (8)	1.624 (7)
	1.632 (4)	1.600 (9)	1.629 (6)
dihedral angle between MNC(···M) planes	37.5	73.0	87.4
twist angle between B and N planes	18.7	18.4	23
asym in NBC angles	16.7	15.9	18.8
color	green	green	dark red

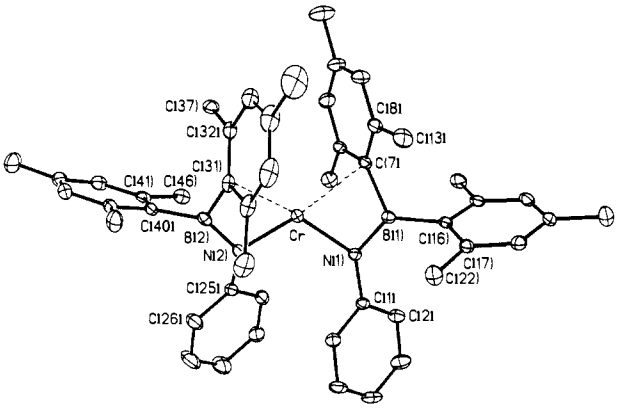

Figure 3. Thermal ellipsoid plot of $Cr(NPhBMes_2)_2$ (**5**). H atoms are omitted for clarity. See Table II for details.

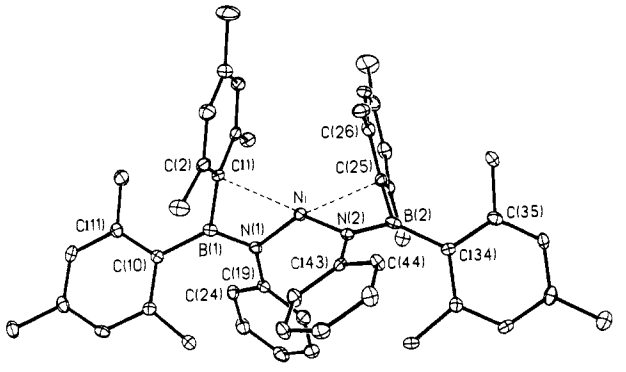

Figure 4. Thermal ellipsoid plot of $Ni(NPhBMes_2)_2$ (**7**). H atoms are omitted for clarity. See Table II for details.

between 1.407 (2) and 1.36 (1) Å, the shorter distances being found for the lithium salts. They are thus consistent with significant p-p overlap in the B-N bond. The Li ions in **3** and **4** are bound to two Et_2O molecules in addition to the nitrogen of the amide. The Li centers are approximately planar, and the angles are irregular owing to the considerable difference in size between the substituents. There is also asymmetry in the NBC angles in all compounds with the smaller angle on the same side as the H or $Li(Et_2O)_2$ substituent. The magnitude of the asymmetry varies between 3.7° and 10.7°.

$M(NPhBMes_2)_2$ (M = Cr, 5; Co, 6; Ni, 7). Each structure consists of well-separated monomers. Structural details are provided in Table II. The three compounds all display large deviations from linearity. The NMN bending is greatest for chromium (Figure 3) and least for nickel (Figure 4). In addition

(25) Covalent radii estimated from homonuclear bond lengths: Sutton, L. Ed.; Tables of Interatomic Distances and Configuration in Molecules and Ions. *Spec. Publ.—Chem. Soc.* **1958**, *No. 11*; *Spec. Publ.—Chem. Soc.* **1965**, *No. 18*. Slater, J. C. *J. Chem. Phys.* **1964**, *41*, 3199.

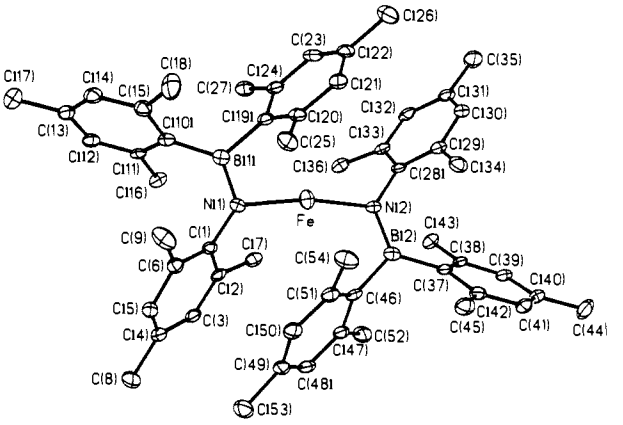

Figure 5. Thermal ellipsoid plot of $Fe(NMesBMes_2)_2$ (**10**). H atoms are omitted for clarity. See Table III for details.

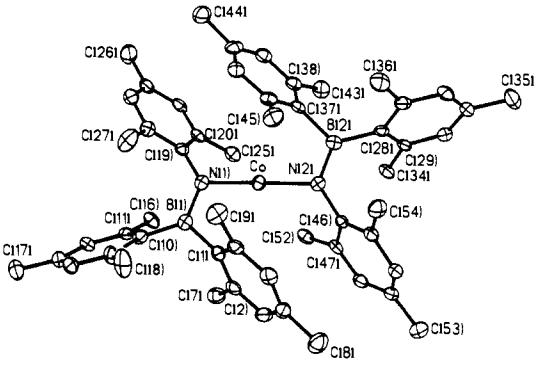

Figure 6. Thermal ellipsoid plot of $Co(NMesBMes_2)_2$ (**11**). H atoms are omitted for clarity. See Table III for details.

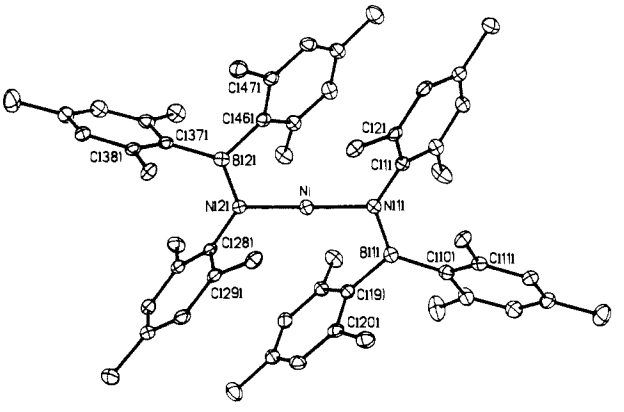

Figure 7. Thermal ellipsoid plot $Ni(NMesBMes_2)_2$ (**12**). H atoms are omitted for clarity. See Table III for details.

to the primary coordination of the metal to two nitrogens, there are fairly close interactions (2.3–2.4 Å) between the metals and one ipso carbon from each $-BMes_2$ group. Within the ligands there are large asymmetries (16–19°) in the N–B–C angles. In addition, there are significant differences (0.03–0.04 Å) in the two B–C bond lengths in the $-BMes_2$ groups, with the longer distance being associated with the M···C interaction. These are grounds for viewing the coordination of the metals as distorted pseudotetrahedral in the case of **6** and **7** and pseudo square planar for **5**. This view is further underlined by the large dihedral angles between the MNC(···M) planes. The B–N distances within each ligand are all near 1.4 Å and are consistent with B–N multiple bonding. The nitrogen and boron centers are planar, but they have fairly high twist angles of ca. 20° between the planes.

$M(NMesBMes_2)_2$ (M = Cr, 8; Mn, 9; Fe, 10; Co, 11; Ni, 12). Important structural data for compounds **8–12** are provided in Table III. The compounds crystallize as well-separated molecular monomers of formula $M(NMesBMes_2)_2$ with no close intermolecular contacts. The crystals of **10–12** are isomorphous, un-

Table III. Important Bond Distances (Å) and Angles (deg) and Other Structural Parameters for $M(NMesBMes_2)_2$ (M = Cr → Ni)

	Cr, **8**	Mn, **9**	Fe, **10**	Co, **11**	Ni, **12**
N-M-N	112.3 (3)	160.4 (2)	166.6 (1)	168.4 (1)	167.9 (1)
M-N (av)	1.984 (7)	2.046 (4)	1.938 (2)	1.910 (3)	1.866 (2)
M···C (<2.8 Å)	2.383	2.536	2.521	2.629	2.611
	2.391			2.734	2.703
B-N (av)	1.377 (12)	1.402 (7)	1.409 (4)	1.406 (6)	1.412 (4)
B-C	1.598 (14)	1.603 (8)	1.592 (4)	1.598 (5)	1.595 (3)
	1.624 (14)		1.598 (4)	1.592 (5)	1.596 (3)
			1.607 (5)		
B-C(···M)	1.647 (14)	1.618 (8)	1.622 (5)	1.612 (6)	1.617 (4)
	1.646 (14)			1.624 (7)	1.619 (4)
dihedral angle between MNC(···M) planes	18.7	45.8			
twist angle between B and N planes	11.1	7.5	3.7	2.8	2.4
asym in NBC angles	14.8	13	12.3	13.1	13.6
color	turquoise	pale pink	pale amber	dark red	dark red

derlining their structural similarity (see Figures 5 and 6 for the structures of **10** and **11**), whereas molecules of solvent are included in the lattice of **9** and the distortions seen in the structure of **8** are apparently sufficient to effect a change in crystal morphology. None of the compounds possess a linear N-M-N unit although in the iron, cobalt, and nickel (Figure 7) compounds the deviations from this geometry are relatively minor, ~13°, while for **9** the NMnN angle is 160.4 (2)° and for the Cr compound **8** it is 112.3 (3)°. The M···C interactions in **9–12** vary from 2.521 to 2.734 Å and are much longer than the corresponding distances in the $-NPhBMes_2$ compounds **6** and **7**. In addition, the asymmetry in the NBC angles in **9–12** is about 13°, which is significantly less than that seen in **5–7**. Furthermore, the differences in length between the B-C bonds in the mesityl groups are marginal and vary from 0.015 to 0.023 Å for the series **9–12**. In effect, the metals in **9–12** are essentially two-coordinate since the metal interactions with the ipso carbons of the boron mesityl groups are extremely weak. In contrast, much stronger distortions were observed for the $Cr(NMesBMes_2)_2$ species **8**. With a N-Cr-N angle of 112.3 (3)° and Cr···C interactions of 2.383 and 2.391 Å, the environment at Cr in **8** more closely resembles that of $Cr(NPhBMes_2)_2$ rather than species **9–12**. Interestingly, the largest asymmetry in the B-C bonds was also observed in **8** although the standard deviations in the bond lengths are too high for this to be of great significance. The twist angles between the boron and nitrogen planes are in all cases small, varying between 6 and 13°.

Discussion

Amide ($-NR_2$) ligands have, thus far, proved to be the most versatile in the stabilization of low coordination numbers among the transition elements.[26,27] This is due to a favorable combination of thermodynamic (strong M-N bonds) and steric factors (two R groups can be varied in size) that allow the synthesis of compounds with fairly high stability. It has been shown that the $-N(SiMe_3)_2$,[26] $-N(i\text{-}Pr)_2$,[28] and $-NPh_2$[4,29] groups are particularly apt for the stabilization of three-coordinate compounds. The $-N(SiMe_3)_2$ ligand has been the most widely studied, and although it is also capable of giving stable divalent species, which are monomeric in the vapor,[6] these compounds are clearly unsaturated. For example, they dimerize in the solid[7,13,14] and form adducts such as $Co\{N(SiMe_3)_2\}_2(PPh_3)$[30] or $Fe\{N(SiMe_3)_2\}_2(py)_2$.[31] In order to synthesize stable unassociated two-coordinate open-shell transition-metal compounds, two strategies have been followed in this laboratory. First, silylamide ligands were modified to include larger substituents as in $-N(SiMe_nPh_{3-n})_2$ (n = 0, 1, 2), which allowed the synthesis of crystalline, two-coordinate Mn(II), Fe(II), and Co(II) derivatives.[5] Second, noting the stability of the $-NPh_2$ derivatives, a diarylboryl group ($-BMes_2$, $-BXyl_2$) was substituted for one of the phenyl rings in $-NPh_2$. The objective was the reduction of the bridging tendency of the nitrogen lone pair through π-bonding with boron.[32] The results from the first approach have been described in detail elsewhere.[5,33] The currently available data arising from the second approach are discussed here. It is of interest to note that these borylamide ligands are the BN analogues of alkenyls. Transition-metal alkenyls have received less attention than alkyls, and only a few homoleptic derivatives have been well characterized.[34]

The syntheses of the precursors and compounds **5–12** were relatively straightforward and afforded moderate to excellent yields of the products. It was found to be convenient, in the case of the Cr, Mn, and Ni species, to use tetrahydrofuran solvate precursors that were synthesized by overnight Soxhlet extraction of finely ground salts $CrCl_2$, $MnBr_2$, and $NiBr_2$. Satisfactory results were obtained in the case of Fe and Co with $FeBr_2$ and $CoCl_2$ that have significant solubility in ether solvents. The transition-metal compounds **5–12** are extremely air and moisture sensitive and were handled accordingly.

Structures. The salient features of the structures of **1–12** have been outlined above. The structures of **1** and **2** need little further comment except to note that they are quite normal and possess no features that have not already been seen in the structures of other aminoboranes. The structures of the lithium salts **3** and **4** are notable because of their monomeric character. Normally, lithium amides are associated even when they involve sterically crowding substituents such as $-N(SiMe_3)_2$[25,36] or 2,2,6,6-tetramethylpiperidine. Monomeric structures for lithium amides have only been recently observed when multidentate or macrocyclic solvent ligands are used to coordinate Li or when very large substituents $-N(SiMePh_2)_2$ or $-N(SiPh_3)_2$ were used.[33] It is notable that the B-N distances in **3** and **4** are significantly shorter than those in **1** or **2**. This is presumably due to the greater negative charge on nitrogen that enhances B-N π-bonding. The asymmetry in the NBC angles is also notable in view of the significance of this parameter on the transition-metal species; vide infra. In the context of the data available on the transition-metal species and

(26) Bradley, D. C. *Chem. Ber.* **1975**, *11*, 393. Chisholm, M. H.; Bradley, D. C. *Acc. Chem. Res.* **1976**, *9*, 273.
(27) Eller, P. G.; Bradley, D. C.; Hursthouse, M. B.; Meek, D. W. *Coord. Chem. Rev.* **1977**, *24*, 1. Lappert, M. F.; Power, P. P.; Sanger, A. R.; Srivastava, R. C. *Metal and Metalloid Amides*; Ellis Horwood: Chichester, England, 1980.
(28) Bradley, D. C.; Hursthouse, M. B.; Rodesiler, P. F. *J. Chem. Soc., Chem. Commun.* **1969**, 14.
(29) Dermer, O. C.; Fernelius, W. C. Z. *Anorg. Allg. Chem.* **1935**, *221*, 83. Frölich, H. O.; Märkisch, V. *Z. Chem.* **1975**, *15*, 276. Brito, V.; Frölich, H. O.; Müller, B. *Z. Chem.* **1979**, *19*, 28. Frölich, H. O.; Römhild, W. *Z. Chem.* **1980**, *20*, 154.
(30) Bradley, D. C.; Hursthouse, M. B.; Smallwood, R. J.; Welch, A. J. *J. Chem. Soc., Chem. Commun.* **1972**, 872.
(31) Power, P. P.; Shoner, S. Unpublished results, 1989.
(32) However, this approach does not always prevent bridging as in the dimers $[M\{NB(Et)C(Et)C(Me)SiMe_2\}_2]_2$ (M = Fe, Co); see: Köster, R.; Seidel, G.; Boese, R.; Wrackmeyer, B. *Chem. Ber.* **1987**, *120*, 669.
(33) Chen, H.; Bartlett, R. A.; Dias, H. V. R.; Olmstead, M. M.; Power, P. P. *J. Am. Chem. Soc.* **1989**, *111*, 4338.
(34) Cardin, C. J.; Cardin, D. J.; Kelly, J. M.; Norton, R. J.; Roy, A. *J. Organomet. Chem.* **1977**, *132*, C23-C25. Cardin, C. J.; Cardin, D. J.; Roy, A. *J. Chem. Soc., Chem. Commun.* **1978**, 399. Cardin, C. J.; Cardin, D. J.; Morton-Blake, D. A.; Parge, H. E.; Roy, A. *J. Chem. Soc., Dalton Trans.* **1987**, 1641.
(35) Lappert, M. F.; Slade, M. J.; Singh, A.; Atwood, J. L.; Roger, R. D.; Shakir, R. *J. Am. Chem. Soc.* **1983**, *105*, 302.
(36) Engelhardt, L. M.; May, A. S.; Raston, C. L.; White, A. L. *J. Chem. Soc., Dalton Trans* **1983**, 671.

related structures, several other points can be made:

(a) None of the structures exhibit bridging through nitrogen even though bulky amide ligands such as $-N(SiMe_3)_2$ and $-NPh_2$ form bridges in closely related species.

(b) In all compounds the B–N bond lengths are consistent with π-bonding between boron and nitrogen. The neutral ligands are thus B–N analogues of the alkenyls and behave, for the most part, as one-electron donors. Compounds **5–12** are therefore extremely electron poor. For example, the chromium species **5** and **8** formally possess only 8 electrons in their valence shells. The most electron-rich nickel compounds, **7** and **12**, have 12 valence electrons.

(c) All the transition-metal compounds show deviation from linearity in the N–M–N unit. This deviation is greatest for the $-NPhBMes_2$ derivatives **5–7**. For the $-NMesBMes_2$ compounds only Cr species **8** displays distortions of similar magnitude.

(d) Asymmetry in the N–B–C angles, which may be an indicator of the amount of M···C interaction, is observed in all compounds. Moreover, it is greatest (~16–19°) in the transition-metal $-NPhBMes_2$ derivatives and **8**. It is significantly less (~13°) in the $-NMesBMes_2$ compounds **9–12** and least (3.7–10.7°) in precursors **1–4**. It is, however, noteworthy that the amount of asymmetry (10.7°) in the lithium salt of the $-NMesBMes_2$ ligand is only marginally (2–3°) smaller than that seen in its transition-metal derivatives **9–12**. This is in agreement with the small deviations from linearity in the NMN moiety (point c), the weak M–C interactions (Table III), and almost negligible differences in the B–C bond lengths (point e, vide infra).

(e) The asymmetry in the B–C bond lengths also roughly parallels the angular deviations. There are negligible differences in **1–4**. In the $-NMesBMes_2$ species **9–12** they vary between 0.015 and 0.023 Å. Such variations can have only marginal significance in view of the magnitude of the standard deviations in these parameters. In the $-NPhBMes_2$ compounds more substantial differences (up to 0.046 Å) were observed. See Tables I–III for more details.

(f) The M–N bond lengths in the $-NPhBMes_2$ and $-NMesBMes_2$ transition-metal complexes parallel the expected decrease in ionic radius for high-spin M^{2+} ions proceeding from left to right across the first transition series. Furthermore, the M–N bond lengths in **6** and **9–11** are close to those found in the crystalline $M[N(SiMePh_2)_2]_2$ (M = Mn, Fe, and Co complexes). No structural data on other bivalent monomeric Cu(II) and Ni(II) (Figure 7) amides are currently available although the structures of the closely related dimers $[Ni(NPh_2)_2]_2$[16] and $[Cr\{N(i\text{-}Pr)_2\}_2]_2$[37] are now known.

These points imply the following:

(i) Intermolecular association in **2–12** is not observed because the nitrogen lone pair is unavailable due to B–N π-bonding. Instead, intramolecular association occurs to a degree permitted by the size of the metal ion and the nitrogen substituent.

(ii) The transition-metal species can be divided into two categories: first are the species **5–8** that show significant structural manifestations of the interaction between an ipso carbon and the metal, and second are the compounds **9–12** that display much less pronounced distortions. The origin of the distortion from linearity in both classes of compound can be attributed to the electron deficiency of the metal centers and their tendency to seek electron density in the aromatic substituents of the ligands. The degree of departure from a linear geometry can be approximately correlated to the degree of electron deficiency at the metal center, although steric factors also play a role (vide infra).

(iii) The secondary M···C interactions, even when they are relatively strong, appear to have little or no effect on the M–N bond lengths. The M–N bonds are close to the estimated length for two-coordination and do not show any lengthening that might be expected upon a possible increase in the coordination number of the metal to four as in **5–8**. For example, the Cr–N bonds in **5** and **8** average 1.983 Å in length, however in the four-coordinate complex *trans*-$[Cr\{N(SiMe_3)_2\}_2(THF)_2]$[15] the Cr–N bonds are 2.089 (10) Å. The only instance in which it is possible to argue that the M–N distance is somewhat lengthened is in Mn species **9**. Here the Mn–N bond 2.046 (4) Å is close to that found (2.023 (3) Å) in the three-coordinate species $[Li(THF)Mn\{N(SiMe_3)_2\}_3]$[14] rather than the values in the two-coordinate $Mn[N(SiMePh_2)_2]_2$[23] 1.989 (3) Å, or 1.95 (2) Å found in the vapor electron diffraction study of $Mn[N(SiMe_3)_2]_2$[6], or the terminal Mn–N bond, 1.998 (3) Å, in the weakly associated dimer $[Mn\{N(SiMe_3)_2\}_2]_2$.[13,14] Comparison of structural data[33] for the iron and cobalt complexes with the structures of $M[N(SiMePh_2)_2]_2$, Fe–N = 1.917 (2) Å and Co–N = 1.901 (2) Å, indicates that the differences between these numbers and those for **6**, **7**, and **10**, and **11** are slight.

A striking feature of the structural data for the transition-metal species is the large difference observed between the $-NPhBMes_2$ and $-NMesBMes_2$ derivatives of cobalt and nickel whereas the chromium derivatives have very similar structures. These differences may be accounted for in terms of the disparity in size between the two ligands and the relative sizes of the metals. Both cobalt and nickel are significantly (~0.1 Å) smaller than chromium.[25] It is therefore much easier for the M···C interaction to occur in chromium because its large size permits a closer approach of the boron mesityl groups. The cobalt and nickel atoms are apparently too small to allow a similar interaction when mesityl is substituted for the phenyl group or nitrogen. However, the presence of the smaller phenyl group reduces the crowding sufficiently for significant M···C interaction to occur in **6** and **7**.

There are a number of other structural features unique to the chromium complexes. For example, the crowding in $Cr(NMesBMes_2)_2$ (**8**) is manifested by distortions involving the interacting mesityls that are inclined away from the Cr center so that the angles between B(1)C(10) and B(2)C(37) bonds and the respective ring planes are 10.2 and 15.2°. Also, there is a fairly small (18.7°) dihedral angle between the two CrNC planes. In effect, the geometry at Cr in **8** is nearer to square-planar than tetrahedral. This interesting arrangement is presumably a result of its high-spin d^4 electron configuration. The "square-planar" coordination in **8** is all the more remarkable because the larger mesityl substituents on nitrogen should favor a more tetrahedral-like configuration to reduce crowding. The low dihedral angle may be contrasted with the values of 71.7° and 87.4° found for **6** and **7** that have pseudotetrahedral geometry at Co and Ni.

The data in Tables II and III also exhibit some other interesting trends. For example, there is a tendency toward increased B–N bond lengths in the later metals. This implies that the B–N bond order is decreased in the nickel compounds compared to chromium analogues. In addition, there is no correlation between this trend and the twist angles between the B and N planes. One possible explanation is that the B–N bonds on the right-hand side are longer because the more electron-rich metals such as nickel can donate electron density more effectively into a B–N π^*-orbital than chromium. An alternative explanation (and the more likely one in view of low numbers of valence electrons in **5–12**) is that, owing to the larger size of Cr, the ionic character of Cr–N bond in **5** or **8** is greater, which in turn leads to a stronger B–N π-interaction in much the same way as the B–N bonds in **3** or **4** are shorter than those observed in **1** or **2**.

Table IV. Electronic Absorption Spectra of $M(NRBMes_2)_2$ (M = Cr, Co, Ni; R = Ph, Mes) (cm^{-1}) with ϵ Values in Parentheses

	Cr	Co	Ni
$M(NMesBMes_2)_2$	12530 (77)	12580 (50)	17420 (914)
	16030 (252)	12820 (31)	23040 (1100)
		16000 (76)	28980 (1200)
$M(NPhBMes_2)_2$	12350 (36)	15240 (78)	16670 (sh)
	14880 (54)	16400 (89)	20330 (1300)
		20010 (95)	
		24290 (386)	

Electronic Absorption Spectra. Solutions of the Cr, Co, and Ni complexes in toluene all show significant absorptions in the UV/vis region as summarized in Table IV. It was noted in the

(37) Edema, J. J.; Gambarotta, S.; Spek, A. L. *Inorg. Chem.* **1989**, *28*, 812.
(38) Pople, J. A.; Schneider, W. G.; Bernstein, H. J. *High Resolution Nuclear Magnetic Resonance*; McGraw-Hill: New York, 1959; p 367. Kost, D.; Carlson, E. H.; Raban, M. *J. Chem. Soc., Chem. Commun.* **1971**, 656.

Table V. Magnetic Moments (μ_B) of Compounds 5–12[a]

$M(NPhBMes_2)_2$: Cr (5), 4.91; Co (6), 4.11; Ni (7), 3.91	
$M(NMesBMes_2)_2$: Cr (8), 4.92; Mn (9), 5.98; Fe (10), 4.92; Co (11), 4.36; Ni (12), 2.9	

[a] Determined in C_6H_6/C_6D_6 solution via the Evans method.[18]

structural discussion that there are considerable differences between the structures of the Co and Ni derivatives of the $-NPhBMes_2$ and $-NMesBMes_2$ ligands whereas chromium compounds **5** and **8** have broadly similar structures. The absorption spectra appear to confirm this pattern. This is particularly true in the case of cobalt where **6**, **6a**, and **6b** (all green) and **11** (dark red) have different colors. The spectra of nickel species **7** and **12** also differ markedly in terms of the number, intensity, and energy of the absorptions. In contrast, chromium species **5** and **8** have similar patterns, with the lowest energy absorption appearing at almost identical energies whereas the higher energy absorption differs by about 1100 cm^{-1}.

The ground states for Cr^{2+}, Co^{2+}, and Ni^{2+} are ^5D, ^4F, and ^3F. If, in solution, an approximate two-coordinate geometry is assumed for the cobalt and nickel derivatives (**11** and **12**) of the $-NMesBMes_2$ ligand, then, for **11**, the three transitions could be $^4\Sigma_g^- \rightarrow {}^4\Pi_g(P)$, $^4\Sigma_g \rightarrow \Sigma_g(P)$, and $^4\Sigma_g \rightarrow {}^4A_g(F)$ in order to decreasing energy. In the case of the cobalt–$NPhBMes_2$ derivative the symmetry should be lowered to C_{2v} due to the strong Co···C interaction. The relative energy of the bands should also change. A stronger effective ligand field splitting probably can be expected as a result of the extra coordination. The shift to higher absorption energies between **6** and **11** is in qualitative agreement with these arguments. In a similar manner the closely related structures of the two chromium compounds have similar spectra. The ligand field of approximate C_{2v} symmetry (approximately cis square planar) affords a $^5A_1(D)$ ground state that could undergo d–d transitions to the $^5B_1$ and $^5B_2$ states of approximately equal energy and to the higher $^5A_1$ and $^5A_2$ states also close in energy. This very simplistic picture would give rise to the two absorptions observed in **5** and **8**. The absorption bands observed for nickel compounds **7** and **12** also show significant differences. Three bands are observed in the case of **12**, and the highest energy bands may be due to ligand to metal charge transfer owing to their high absorption coefficients. In the case of **7** only one major absorption is observed at 20 330 cm^{-1} with a relatively high intensity (ϵ = 1300). This band has a shoulder at 16 670 cm^{-1}.

Magnetism and NMR Studies. The ^1H NMR spectra of **5–12** all display isotropically shifted peaks as a result of the presence of unpaired electrons. However, no paramagnetically shifted peaks were observed in the case of manganese species **9** presumably due to the broadness of the resonances. ^1H NMR spectra of Mn(II) compounds are often difficult to observe owing to slow electron exchange that causes rapid relaxation. In addition, the magnetic moments of all compounds were determined by the Evans method.[18] These values are provided in Table V. In all cases they are consistent with a high-spin configuration for each ion. This is to be expected in view of the two-coordinate or quasi-two-coordinate geometry of the compounds that give rise to a relatively weak ligand field. The values for the magnetic moment are, with the exception of the Mn species, greater than the spin-only value, indicating that there is a significant orbital contribution to the magnetic moment.

The ^1H NMR spectra of **5–8** and **10–12** feature a number of isotropically shifted peaks. Complete assignments are not possible for all compounds without extensive isotopic labeling and/or substitution studies. The major objective in studying the ^1H NMR spectra was to obtain an estimate of the energy involved in the M···C interaction. The ^1H NMR of cobalt derivatives **6**, **6a**, and **6b**, and **11** and nickel compounds **7** and **12** were studied for this purpose. For the compounds $M(NMesBMes_2)_2$ (M = Co, **11**; Ni, **12**) no dynamic processes were evident in the spectra recorded between ambient temperature and −80 °C. The variable-temperature ^1H NMR spectrum of **12**, illustrated as a stacked plot in Figure 8, displays only the expected chemical shift and peak-broadening variations with temperature. In contrast, the variable-temperature ^1H NMR study of **6**, **6a**, **6b**, and **7** reveals that dynamic processes are occurring that can be "frozen out" by lowering the temperature. The variable-temperature ^1H NMR spectrum of **6** is illustrated in Figure 9. The ^1H NMR of $-BXyl_2$ derivative **6a** was broadly similar to that of **6**. The major difference was the absence of two peaks in **6a** in the 25–45 ppm mesityl region at −50 °C. This enabled assignment of the "extra" two peaks observed in **6** at 30 and 33 ppm to the *p*-methyl groups of the mesityl rings. These two peaks arose from a broad singlet at 297.56 K that split into two peaks at ca. −25 °C. Substitution of the appropriate parameters, $\Delta\nu$ = 2665 (measured 20 °C below T_c) and T_c = 248 K, into the relevant equations reveals that the barrier to this dynamic process is about 10 kcal mol^{-1}. It is thus possible to say that the Co···C interaction cannot have a value in excess of this figure. It is, however, notable that the 10 kcal mol^{-1} figure is a considerable amount of energy and, in this respect, is in agreement with the structural findings for **6**, **7**, and **8** that show close M···C interactions. Returning to the ^1H NMR spectrum of **11**, it is also found to be in agreement with the assignments from the NMR data for **6** and **6a**. The peaks in the key 25–45 ppm region showed no splitting at temperatures as low as 192 K. This is what is expected if one of the mesityl groups on each $-BMes_2$ does not interact very strongly with the cobalt.

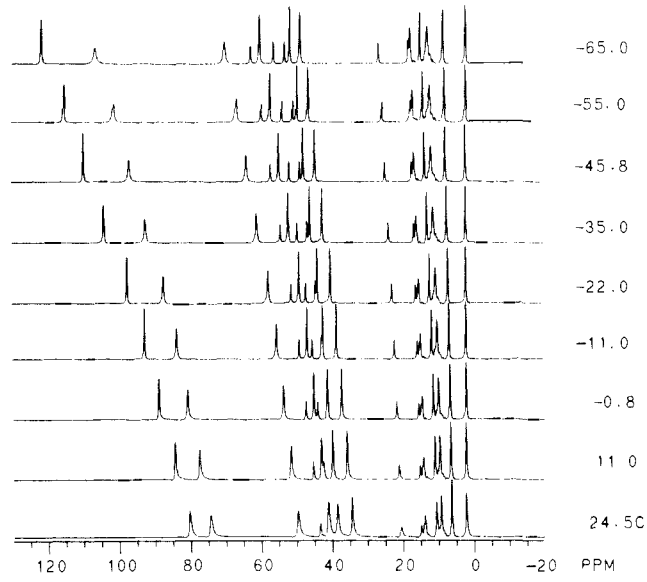

Figure 8. Variable-temperature ^1H NMR data for $Ni(NMesBMes_2)_2$ (**12**) in C_7D_8.

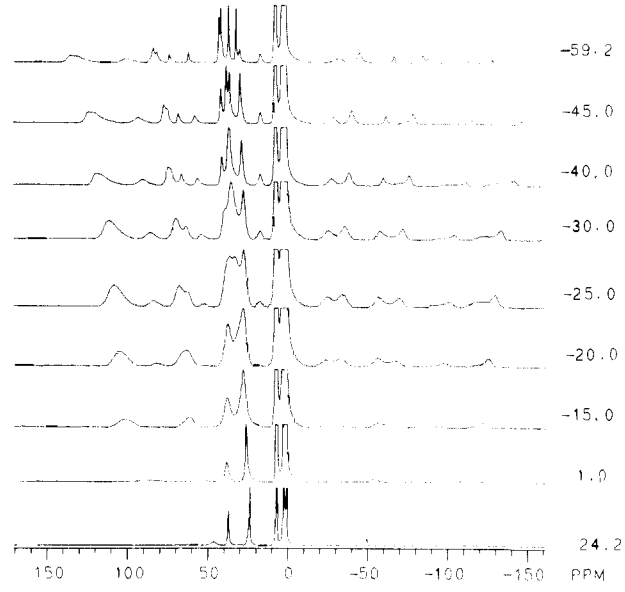

Figure 9. Variable-temperature ^1H NMR data for $Co(NPhBMes_2)_2$ (**6**) in C_7D_8.

Table VI. ^{1}H NMR Data for **6**, **6a**, and **6b** in C_7D_8 at 24.8 °C

	$Co(NPhBMes_2)_2$ (**6**)	$Co(NPhBXyl_2)_2$ (**6a**)	$Co[N(C_6D_5)BMes_2]_2$ (**6b**)
$-BMes_2$	46.1 (*m*-H)	47.2 (*m*-H)	46.2 (*m*-H)
	36.8 (*p*-Me)	-112.6 (*p*-H)	36.9 (*p*-Me)
	23.4 (*o*-Me)	23.1 (*o*-Me)	23.4 (*o*-Me)
-NPh	~24.5	31.2	
	0.2	0.4	
	49.9	-48.6	

Unambiguous assignment of the peaks in the spectra of **6** and **6a** is possible with the use of the deuterated derivative **6b**. Inspection of the data in Table VI reveals peaks due to the $-BMes_2$ group that are common to the three compounds. In addition, the deuterated phenyl group confirms the assignment of the remaining peaks in **6** and **6a** to the phenyl substituent.

In summary, a series (Cr → Ni) of transition-metal borylamides have been described. Though they are nominally two-coordinate, they will intramolecularly associate through a boron-mesityl ipso-carbon if permitted by either iess sterically demanding nitrogen substituents or larger metallic radii. The intramolecular association is caused by the electron deficiency of the metals and the availability of electron density elsewhere in the molecule. The energy of this association is about 10 kcal in the case of cobalt species **6** and presumably **5** and **7**. With bulkier mesityl groups on nitrogen, two-coordination is observed for the metal series Mn → Ni. The chemistry of these interesting compounds is currently under investigation.

Acknowledgment. We thank the National Science Foundation (Grant CHE-8618739) and the donors of the Petroleum Research Fund, administered by the American Chemical Society, for financial support.

Supplementary Material Available: Full tables of crystallographic data, summary of data collection and refinement, positional parameters for non-hydrogen atoms, bond distances and angles, anisotropic thermal paramaters, and hydrogen coordinates (51 pages). Ordering information is given on any current masthead page.

Metal Template Assisted Schiff Base Condensations: An Evaluation of Thermodynamic versus Kinetic Control

Daniel J. Sheeran and Kristin Bowman Mertes*

Contribution from the Department of Chemistry, University of Kansas, Lawrence, Kansas 66045.
Received February 24, 1989

Abstract: The influence of kinetic and thermodynamic template effects has been examined for a unique platinum(II) complex, Pt(AAA)Cl (I) (AAA = *N*-(*o*-aminobenzylidene)anthranilaldehyde), resulting from the Schiff base condensation of two molecules of *o*-aminobenzaldehyde with $PtCl_4^{2-}$. The photochromic behavior of the terminal aldehyde of the dimeric condensate, I, which is replaced by coordinating solvents in the absence of light, allowed for the examination of the role of the metal ion in Schiff base condensations. New compounds were synthesized from I and 1,2-diaminobenzene, 1,2-diaminoethane, 1,3-diaminopropane, *o*-aminobenzylamine, *o*-toluidine, *o*-methylbenzylamine, methylamine, and *n*-propylamine. The kinetics of the reactions of three monoamines and two diamines with both I and solvated I (II) were examined. The Schiff base condensation did not occur to an appreciable extent in II, in which the aldehyde was not coordinated to the metal. The k_{obs} of the condensation with I when the aldehyde was coordinated ranged from 0.000165 s^{-1} for *o*-toluidine to 0.172 s^{-1} for methylamine at 25 °C, with aliphatic amines consistently faster than aromatic amines and bidentate amines faster than monodentate amines. Activation parameters were indicative of a bimolecular reaction. Significant secondary deuterium isotope effects were observed, with k_H/k_D ranging from 1.10 to 1.13. The kinetic results are consistent with an initial attack of the amine on the aldehyde carbon, isomerization to an N-coordinated carbinolamine, and a subsequent dehydration step.

Metal ion template assistance has been a boon to the rational design of complex multidentate ligand systems.[1] These reactions are often complicated by undesirable features such as polymerization or multiple product formation. The synthetic utilization of metal ions has been particularly valuable in Schiff base and related condensations.[2] In these reactions an amine and carbonyl react to form a carbinolamine intermediate followed by dehydration, giving an imine product. Unfortunately, these condensations are not normally "well-behaved", and unwanted side reactions often interfere with the isolation of the desired product. It is in this type of situation that metal ions have been so useful in providing a template for directing the course of the reaction. Examination of mechanistic pathways has been undertaken by a number of researchers.[3-7] Nonetheless, the opportunity to study

Scheme I[a]

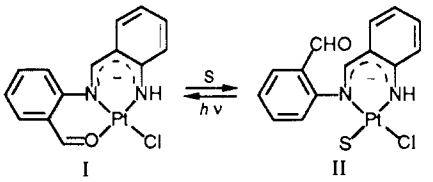

I II

[a] S = solvent.

(1) (a) Busch, D. H. *Rec. Chem. Prog.* **1964**, *25*, 107. (b) Busch, D. H. In *Bioinorganic Chem.*; Gould, R. F., *Ed.*; American Chemical Society: Washington, DC, 1971; p 44. (c) *Synthesis of Macrocycles: The Design of Selective Complexing Agents* (Vol. 3 of *Progress in Macrocyclic Chemistry*); Izatt, R. M., Christensen, J. J., Eds.; Wiley-Interscience: New York, 1987. (d) Curtis, N. F. *Coord. Chem. Rev.* **1968**, *3*, 3. (e) Lindoy, L. F.; Busch, D. H. In *Preparative Inorganic Reactions*; Jolly, W., Ed.; Interscience: New York, 1971; Vol. 6, p 1. (f) Nelson, S. M. *Pure Appl. Chem.* **1980**, *52*, 2461. (g) Fenton, D. E. *Pure Appl. Chem.* **1986**, *58*, 1437. (h) Fenton, D. E. *Chem. Soc. Rev.* **1988**, *17*, 69.

(2) (a) Dwyen, F. P.; Mellor, D. P. *Chelating Agents and Metal Chelates*; Academic: London, 1964. (b) Busch, D. H.; Cairns, C. In *Synthesis of Macrocycles: The Design of Selective Complexing Agents*; Vol. 3 of *Progress in Macrocyclic Chemistry*; Izatt, R. M., Christensen, J. J., Eds.; Wiley-Interscience: New York, 1987; pp 1-51. (c) Lindoy, L. F. *Rev. Chem. Soc.* **1971**, *25*, 379. (d) Haque, Z. P.; McParthn, M.; Tasker, P. A. *Inorg. Chem.* **1979**, *18*, 2920. (e) Black, D. St. C.; Rothnie, N. E. *Aust. J. Chem.* **1983**, *36*, 1149.

(3) (a) Curtis, N. F. *J. Chem. Soc.* **1960**, 4409. (b) Curtis, N. F. *Coord. Chem. Rev.* **1968**, *3*, 3. (c) Morgan, K. R.; Martin, J. W.; Curtis, N. F. *Aust. J. Chem.* **1979**, *32*, 2371.

0002-7863/90/1512-1055$02.50/0